Title

Histopathologies, Immunolocalization, and a Glycan Binding Screen Provide Insights into Plasmodium falciparum Interactions with the Human Placenta1

Journal

Biology of Reproduction, 88(6)

ISSN

0006-3363

Authors

Hromatka, Bethann S
Ngeleza, Sadiki
Adibi, Jennifer J
et al.

Publication Date

2013-06-20

DOI

10.1095/biolreprod.112.106195

Peer reviewed

BIOLOGY OF REPRODUCTION (2013) **88**(6):154, 1–14
Published online before print 10 April 2013.
DOI 10.1095/biolreprod.112.106195

Histopathologies, Immunolocalization, and a Glycan Binding Screen Provide Insights into *Plasmodium falciparum* Interactions with the Human Placenta[1]

Bethann S. Hromatka,[3] Sadiki Ngeleza,[4] Jennifer J. Adibi,[3] Richard K. Niles,[3] Antoinette K. Tshefu,[4] and Susan J. Fisher[2,3]

[3]*Departments of Obstetrics and Gynecology, Anatomy, the Center for Reproductive Sciences, and The Eli and Edythe Broad Center of Regeneration Medicine and Stem Cell Research, University of California, San Francisco, San Francisco, California*
[4]*Kinshasa School of Public Health, Kinshasa, Democratic Republic of the Congo*

ABSTRACT

During pregnancy, *Plasmodium falciparum*-infected erythrocytes cytoadhere to the placenta. Infection is likely initiated at two sites where placental trophoblasts contact maternal blood: 1) via syncytiotrophoblast (STB), a multicellular transporting and biosynthetic layer that forms the surface of chorionic villi and lines the intervillous space, and 2) through invasive cytotrophoblasts, which line uterine vessels that divert blood to the placenta. Here, we investigated mechanisms of infected erythrocyte sequestration in relationship to the microanatomy of the maternal-fetal interface. Histological analyses revealed STB denudation in placental malaria, which brought the stromal cores of villi in direct contact with maternal blood. STB denudation was associated with hemozoin deposition ($P = 0.01$) and leukocyte infiltration ($P = 0.001$) and appeared to be a feature of chronic placental malaria. Immunolocalization of infected red blood cell receptors (CD36, ICAM1/CD54, and chondroitin sulfate A) in placentas from uncomplicated pregnancies showed that STB did not stain, while the underlying villous stroma was immunopositive. Invasive cytotrophoblasts expressed ICAM1. In malaria, STB denudation exposed CD36 and chondroitin sulfate A in the villous cores to maternal blood, and STB expressed ICAM1. Finally, we investigated infected erythrocyte adherence to novel receptors by screening an array of 377 glycans. Infected erythrocytes bound Lewis antigens that immunolocalized to STB. Our results suggest that *P. falciparum* interactions with STB-associated Lewis antigens could initiate placental malaria. Subsequent pathologies, which expose CD36, ICAM1, and chondroitin sulfate A, might propagate the infection.

placenta, pregnancy, stroma, syncytiotrophoblast, trophoblast

INTRODUCTION

Within sub-Saharan Africa, about 25 million women become pregnant annually and are susceptible to infection with *Plasmodium falciparum* [1, 2]. Infection is most common in primigravid and secundigravid women and is associated with infant low birth weight, intrauterine growth restriction, and preterm labor [2, 3]. Maternal complications such as anemia [4] and a preeclampsia-like syndrome [5] also occur. In sub-Saharan Africa, roughly one in four women shows signs of placental infection at the time of delivery [1], though numbers vary depending on geographic location and method of diagnosis. Transplacental transfer of parasites from maternal to fetal blood rarely occurs [6]. Malaria rates peak during the second trimester of pregnancy and decline toward term [7].

The hallmark of placental malaria is the sequestration of infected red blood cells (iRBCs) in the maternal blood spaces of the placenta (i.e., the intervillous space). The anatomy of this region is shown in Supplemental Figure S1 (all Supplemental Data are available online at www.biolreprod.org). Parasite sequestration has been proposed to occur through iRBC interactions with syncytiotrophoblast (STB), intervillous fibrin deposits [8, 9], and/or leukocyte infiltrates [10]. Of these mechanisms, iRBC cytoadhesion to STB should initiate sequestration, while the other interactions likely occur due to pathological changes. Parasite binding to STB is mediated, at least in part, through parasite-encoded variant surface antigens (e.g., PfEMP1) [11]. The PfEMP1 family member VAR2CSA is commonly displayed by placental iRBC isolates [12, 13] and is a potential vaccine candidate [14, 15]. Infected RBCs isolated from the maternal blood spaces of term placentas preferentially bind in vitro to chondroitin sulfate glycosaminoglycans (CS-GAGs) containing the chondroitin sulfate A (CS-A) motif [16, 17], and numerous groups have demonstrated that CS-A and VAR2CSA function as a receptor-ligand pair [18–20]. Pregnant women develop protective VAR2CSA-specific antibodies (Abs) during pregnancy; primigravid women have low levels and are most susceptible to placental malaria and poor birth outcomes, while higher titers are found in multigravidae and correlate with increased infant birth weights [2, 21].

Infected RBC adherence to STB may also be mediated through adsorption of IgG-bound iRBCs to syncytial Fc receptors [22, 23] and through iRBC adhesion to hyaluronic acid (HA) [24]; however, a more recent report found that STB do not express HA [25]. Although iRBCs also sequester in the microvasculature and brain, cytoadherence in these locations is largely mediated by CD36 and ICAM1 on endothelial cells [26, 27]. ICAM1 expression has been demonstrated on STB [10, 28] and endovascular invasive cytotrophoblasts (iCTBs) [29] at term, but there are conflicting reports as to whether placental isolates bind this receptor in vitro [17, 30]. Some placental iRBC isolates adhere to CD36 [17], but it does not appear to be expressed by STB at term [28]. Thus, for some molecules, there is a discrepancy between receptor availability and parasite

[1]Supported by NIH 1R21AI079329-01A1. B.S.H was supported by a fellowship from the National Science Foundation. Presented in part at the 57th annual meeting of the American Society of Tropical Medicine and Hygiene, December 7–11, 2008, New Orleans, Louisiana.
[2]Correspondence: E-mail: sfisher@cgl.ucsf.edu

Received: 7 December 2012.
First decision: 6 January 2013.
Accepted: 29 March 2013.

eISSN: 1529-7268 http://www.biolreprod.org
ISSN: 0006-3363

binding preference. To our knowledge, an analysis of ICAM1 and CD36 expression in placentas of younger gestational ages has not been performed.

Numerous histopathological changes have been observed in *P. falciparum*-infected placentas. Maternal leukocytes, primarily monocytes with some lymphocytes and neutrophils, are mobilized to the intervillous space [31–34] and have been associated with poor outcomes, including low birth weight [31, 34–36]. The monocytes often contain hemozoin [32, 36], a pigmented by-product of *P. falciparum* digestion of hemoglobin. Hemozoin is also observed in intervillous fibrin clots or found free [32, 37] and signifies that the placenta was infected earlier in gestation [38]. Although parasitization of fetal vessels has not been reported [6], there is evidence that malaria infection alters the anatomy of the villi [9, 32, 37–40]. A notable feature is the accumulation of hemozoin within the villi, typically in areas of intravillous fibrinoid necrosis [32, 38–40], and inside STB and mesenchymal cells [9, 32, 33, 39]. Additional changes include increased syncytial knotting [33], loss of microvilli [33], and marked thinning and/or loss of the STB layer (i.e., STB denudation or necrosis) [9, 32, 39]. In most cases, the frequency of these lesions has not been studied, and in general it is not known if they are associated with adverse pregnancy outcomes.

MATERIALS AND METHODS

Ethics Statement

This study was approved by the Kinshasa School of Public Health Ethics Committee and the University of California, San Francisco, Committee on Human Research. Written, informed consent was obtained from all participants. All work was conducted in accord with the Society for the Study of Reproduction's specific guidelines and standards.

Participant Recruitment

Biopsies of normal placentas were obtained from patients undergoing elective terminations of pregnancy (5–22 wk) or from women who had uncomplicated deliveries in San Francisco, California. Biopsies of *P. falciparum*-uninfected and -infected placentas were obtained from term deliveries at the Kingasani Maternity Hospital, Kinshasa, Democratic Republic of the Congo. Women were categorized as either malaria-negative or malaria-positive. Malaria-negative women received antenatal care at the Kingasani Maternity Hospital and intermittent preventative therapy (IPT) (two doses of sulfadoxine pyrimethamine for HIV-negative women and three doses for HIV-positive women) and did not present with symptoms of malaria at the time of delivery. Malaria-positive women did not receive antenatal care at Kingasani Maternity Hospital and presented at this institution at the time of delivery with symptoms of malaria; their IPT status was unknown. Malaria-positive women had the following symptoms: fever, joint and muscle pain, and headache. The diagnosis of malaria was confirmed with a peripheral blood smear test that was collected at the time of delivery. Exclusion criteria for both groups included other pregnancy complications: hypertension, preeclampsia, chorioamnionitis, or maternal anemia. Details on participants are shown in Supplemental Table S1.

Tissue Sampling and Handling

Placentas collected in San Francisco were biopsied and frozen at −80°C as previously described [41]. Biopsies collected in Kinshasa were obtained within 20 min of delivery and transferred to 10% neutral buffered formalin (VWR) 10:1 (ml:gram wet weight). To account for heterogeneity across the maternal-fetal interface, five full-depth biopsies (basal plate to fetal membranes; see Supplemental Fig. S1A) were collected from the center (n = 2) and periphery (n = 3). Biopsies were fixed for 24 h, transferred to 70% ethanol, paraffin embedded, and sectioned (5 μm).

Histology

Thirty-four cases and controls (n = 17 per group) were randomly selected based on the sample sizes of previous studies in which we analyzed the effects of preterm labor or preeclampsia on the basal plate region of the placenta [41]. Hematoxylin and eosin (H&E)-stained sections were examined by light microscopy. Five biopsies per placenta and three randomly chosen fields per biopsy (total scored fields = 15 per placenta) were scored at 400× for the number of (1) iRBCs, (2) hemozoin-containing villi per total number of villi, (3) leukocytes in the intervillous space, and (4) denuded villi per total villi. Denuded villi lacked a complete covering of STB; in some cases, intravillous fibrinoid, which by definition is composed of matrix molecules [6], was associated with regions of denudation. Nucleated cells in the intervillous space were assumed to be maternal leukocytes. In general, there was good agreement among the scores for each of the fifteen 400× fields that were examined per placenta.

Statistical Analyses

Maternal age, parity, birth weight, and gestational age were compared between cases and controls. For continuous parameters, *P* values were based on a *t*-test comparing the means, assuming normal distribution and equal variance. For noncontinuous values, *P* values were based on the Fisher exact test to estimate differences in proportions between the two groups. The descriptive statistics for the infection and histopathological features were calculated using summarized data for the fifteen 400× fields that were analyzed per placenta. For departures from normality in dependent variables, values were log transformed, which allowed them to pass the Kolmogorov-Smirnov test for normality. To assess equal variance, we plotted the residuals and did not observe any departures from the equal variance assumption. Linear regression models were fit to estimate univariate associations. We estimated all associations using linear and log values and compared the two to obtain the best model fit. Unless stated, we reported results on a linear scale. In a separate analysis, cases and controls were categorized according to a well-established grading scheme (not infected, active infection, active-chronic infection, past-chronic infection) [38] and plotted as a function of STB loss (Supplemental Fig. S2). Analyses were carried out using the statistical software package SAS 9.2 (SAS).

Immunolocalization

For immunofluorescence detection, frozen biopsies were cryosectioned (5 μm) and fixed in ice-cold methanol/acetone (2:1) for 5 min, and nonspecific reactivity was inhibited by incubating the sections for 1 h in blocking buffer (1% bovine serum albumin [BSA], 0.1% fish gelatin, 0.1% Triton-X-100, and 0.05% Tween-20). Tissue sections were incubated overnight at 4°C with the following primary monoclonal Abs (mAbs; singly or in combinations): anti-CD36 (185-1G2; 10 μg/ml; Thermo Scientific), anti-ICAM1 (15.2; 20 μg/ml; Thermo Scientific), anti-CS-A (LY111; 20 μg/ml; Seikagaku), anti-CS-A (CS-56; 12 μg/ml; Sigma-Aldrich), anti-CS-A (473HD; 1:100; kind gift of Dr. Andreas Faissner, Ruhr University Bochum, Bochum Germany), anti-4S (2-B-6; 7 μg/ml; Seikagaku), anti-6S (3-B-3; 7 μg/ml; Seikagaku), anti-0S (1-B-5; 7 μg/ml; Seikagaku), anti-Le^x (HI98; 5.0 μg/ml; BD Pharmingen), anti-sLe^x (CSLEX1; 5.0 μg/ml; BD Pharmingen), anti-human cutaneous lymphocyte antigen (HECA-452; 2.5 μg/ml; BD Pharmingen), anti-cytokeratin 7 (OV-TL 12/30; 5 μg/ml; Dako), and a rat anti-cytokeratin 7 (7D3; 1:100; [42]). Anti-GAG Ab specificities are described in Supplemental Figure S3. To control for anti-GAG Ab specificity and to expose stubs, sections were preincubated with chondroitinase ABC (10 mU/μl in 0.1% BSA; Seikagaku) at 37°C for 2 h (Supplemental Fig. S4B). Binding of primary mAbs was detected with fluorescein isothiocyanate- or tetramethylrhodamine isothiocyanate-conjugated, species-specific, secondary Abs (Jackson ImmunoResearch). As controls, irrelevant mouse IgG2a (BioLegend), mouse IgG1 (BioLegend), mouse IgM (eBioscience), rat IgM (BD Pharmingen), or PBS was substituted for the primary Ab (Supplemental Fig. S4A). Sections were mounted with DAPI (4′,6-diamidino-2-phenylindole)-containing Vectashield (Vector Laboratories) and imaged with a Leica CTR5000 upright microscope (Leica Microsystems) or a Leica TCS SP5 confocal microscope (Leica Microsystems) at 20×, 40×, or 100× resolution. The staining pattern of each Ab and sample type was evaluated in three independent experiments.

For histochemical detection, tissue sections were deparaffinized in xylene and rehydrated in a series of graded ethanol solutions. Antigens were retrieved by heating for 30 min at 95°C in 10 mM sodium citrate and 0.05% Tween 20 (pH 6.0). Endogenous peroxidase activity was blocked by incubation in 0.3% H_2O_2 (30 min at room temperature). Signals from native IgG bound to fetal Fc receptors were blocked by incubation with goat or donkey anti-human IgG (1.0 μg/ml; Jackson ImmunoResearch; 1 h at room temperature). To block unoccupied Fc receptors, samples were incubated in 1.5% serum from the species in which the secondary Ab was produced. Tissue sections were incubated overnight at 4°C with the following primary mAbs or polyclonal Abs (pAbs): anti-ICAM-1 pAb (1:10; Cell Signaling), anti-CD36 pAb (1:25; Sigma-Aldrich), anti-Le^x mAb (5.0 μg/ml), anti-sLe^x mAb (5.0 μg/ml), and the GAG-

specific mAbs described earlier. Binding of primary Abs was detected with species-specific, biotin-conjugated, secondary Abs (Jackson ImmunoResearch) plus ABC-peroxidase (Vector Laboratories). The reaction was developed with the 3-amino-9-ethylcarbazole substrate (Vector Laboratories), and sections were counterstained with hematoxylin. For controls, rabbit polyclonal IgG (BD Pharmingen), mouse IgM (BioLegend), or PBS was substituted for the primary Abs (Supplemental Fig. S4C). The staining pattern of each Ab was evaluated in three to six independent experiments. To evaluate hemozoin deposition relative to antigen expression, the sections were viewed with polarized light, which illuminates this pigment [43].

Parasite Culturing and Labeling

P. falciparum line CS2 (MRA-96; Malaria Research and Reference Reagent Resource Center) was cultured in fresh human erythrocytes diluted to a 2% hematocrit with RPMI 1640 supplemented with 25 mM HEPES, 2 mg/ml sodium bicarbonate, 100 μM hypoxanthine, 50 μg/ml gentamycin, and 0.25% Albumax II (Invitrogen). The cultures were maintained in a humidified incubator at 5% CO_2, 5% O_2, and 37°C. PCR-based testing for mycoplasma contamination (Stratagene) was done on a regular basis. Cultures were synchronized according to standard methods [44]. When they reached ~5% parasitemia and the majority were schizonts (~1 wk after thawing), the cells were centrifuged at 10 000 × *g* for 5 min and washed twice with RPMI 1640. Then they were resuspended (1.0×10^{10}/ml) in RPMI 1640 containing 25 nM Mitotracker (Invitrogen) and 0.0025% dimethyl sulfoxide and incubated for 15 min in the culture conditions described above. The labeled cells were centrifuged (10 000 × *g*, 5 min), washed once with RPMI 1640, and resuspended (2×10^{10} cells/ml) in PBS containing 1% BSA.

Mapping Candidate P. falciparum *Carbohydrate Receptors Using Glycan Arrays*

Infected RBCs were screened for adherence to printed glycan microarrays (version 3.1) developed by the Consortium for Functional Glycomics [45, 46]. The array contained 5632 spots of 377 natural and synthetic glycans with amino linkers printed on chemically modified glass slides. Each glycan was printed in 12 spots at 10 μM (six spots) and 100 μM (six spots). As landmarks, 160 spots were printed with biotin, and as controls, 936 spots were empty. The arrays were rehydrated by incubating in 20 mM Tris-HCl, 150 mM NaCl, 2 mM $CaCl_2$, 2 mM $MgCl_2$, and 0.05% Tween 20 for 5 min at room temperature. Mitrotracker-labeled iRBCs/RBCs (1×10^{10}; ~5% parasitemia) in 0.5 mls of PBS + 1% BSA were pipetted onto each array. The iRBC-containing medium also contained 2 μl Cy5-Streptavidin (Zymed), which bound to biotin spots and formed grid coordinates. The iRBC-topped slides were then placed individually in 8 × 12-cm glass boxes and covered. To facilitate interactions with carbohydrate receptors, which often require sheer stress [47], the glass boxes that contained the slides were rotated (40 revolutions per minute) on a 30-cm platform (horizontal) shaker for 30 min at room temperature. Then they were washed twice with 20 mM Tris-HCl, 150 mM NaCl, 2 mM $CaCl_2$, 2 mM $MgCl_2$, air-dried, and imaged using a GenePix Autoloader 4200AL microarray scanner (Axon Instruments) set to 5-μm resolution. Infected RBC adherence was confirmed by microscopy. The entire experiment was performed twice.

The two-color TIFF images were analyzed with SpotReader (version 1.3.1.0; Niles Scientific). The software created a grid of circles superimposed on images of the signals and computed the median intensity for all pixels inside each circle (foreground fluorescence) and in the region surrounding each circle (background fluorescence). Relative fluorescent units (rfu) were computed as the foreground minus background intensity. The data were exported to Excel, and median values were computed for the 12 data points that were collected for each structure. Control spots were analyzed in parallel. The values were normalized by subtracting the mean signal across the entire array and dividing by the standard deviation of the control spot readings. Spots with rfu measurements approximately five-fold higher than the median of all glycan signals and ~50-fold higher than the controls were scored as positive. In general, there was good agreement among the six 100-μM spots for each of the nine glycans that represented the top 3% of all hits (Supplemental Fig. S5). The primary data are available at the Consortium for Functional Glycomics website, http://functionalglycomics.org.

Immunoblotting

STB microvillous membrane preparations were isolated as previously described [48], with minor modifications. Briefly, placental chorionic villi were manually dissected into 5- to 10-mm pieces, resuspended in ice-cold PBS containing a protease inhibitor cocktail (Pierce), and stirred for 1 h. The samples were passed through a 70-μm filter, and the membrane fraction was isolated by a series of centrifugation steps: 1000 × *g* (10 min), 14 000 × *g* (20 min), and 100 000 × *g* (1 h). Pellets were resuspended in PBS and dispersed by repeated aspiration with a 26-gauge needle. Protein concentrations were determined by using the Bradford assay (Bio-Rad). STB preparations (40 μg per lane) were separated on 3%–8% NuPAGE Tris-Acetate gels in Tris-Acetate SDS buffer (Invitrogen) and transferred to nitrocellulose (Bio-Rad). Nonspecific reactivity was blocked by incubating the transfers for 1 h in PBS containing 0.05% Tween 20 (PBST) and 5% nonfat dried milk (blocking buffer). Blots were incubated overnight at 4°C with the following mAbs: anti-Le^x (4.0 μg/ml), anti-sLe^x (4.0 μg/ml), anti-Le^y (F3; 1:250; Abcam), anti-Le^b (LWB01; 1.2 μg/ml; NeoMarkers), anti-Le^a (LWA01; 1.2 μg/ml; NeoMarkers), HECA-452 (2.0 μg/ml), or MECA-79 (2.0 μg/ml; BD Pharmingen). After washing three times for 5 min in PBST, the transfers were incubated for 1 h at room temperature with peroxidase-conjugated, species-specific, secondary Abs (1:2500; Jackson ImmunoResearch). Finally, they were washed three times for 5 min in PBST, and Ab reactivity was detected with ECL Plus (GE Healthcare).

RESULTS

STB Loss Is a Prominent Feature of Placental Malaria

Control term placentas had the expected cellular composition, i.e., a villous core composed of stromal cells and fetal blood vessels completely surrounded by a covering of STB (Fig. 1A). The intervillous space contained primarily free-floating RBCs. At this magnification (400×), approximately one leukocyte per field was observed. At least three previous studies described STB loss in placental malaria [9, 32, 39], but there has not been a systematic attempt to determine whether these changes are focal or widespread. Analysis of multiple sites at various depths showed that infected placentas commonly displayed loss of the STB covering, which brought villous cores into direct contact with the intervillous space. Villous cores either resembled normal stroma or were largely acellular and eosinophilic, consistent with intravillous fibrinoid (i.e., subsyncytial fibrinoid or villous fibrinoid necrosis) that is composed of extracellular matrix molecules and fibrin [6]. The exposed regions were often reservoirs for iRBCs and maternal leukocytes. Hemozoin-containing cells with the morphological appearance of monocytes were commonly observed (Fig. 1D). In many cases iRBCs were found in close proximity to the exposed villous stroma (Fig. 1E). Within the lesioned villi, hemozoin deposits (Fig. 1F) were commonly observed in acellular regions that lacked nuclei. These results showed that in placental malaria, dramatic morphological alterations bring maternal blood in direct contact with the villous cores.

STB Loss Is associated with Markers of Infection and Inflammation

We quantified the observed pathologies (Supplemental Table S2) to determine if STB denudation was focal or widespread and to investigate if it correlated with markers of infection and inflammation. The mean percentage of villi displaying regions of STB denudation was 2.2-fold higher in *P. falciparum*-infected versus control samples (SEM = 1.2, $P < 0.0001$; Fig. 2A). The observed range was 10.0%–39.0% for *P. falciparum*-infected and 3.0%–13.0% for uninfected placentas (Supplemental Table S2). The mean number of maternal leukocytes per field was 18% higher in malaria-infected versus control samples (SEM = 7.0%, $P = 0.01$; Fig. 2B). The observed range was 14.6–128.0 for *P. falciparum*-infected and 8.6–30.5 for uninfected placentas (Supplemental Table S2). In infected samples, the mean percentage of hemozoin-containing villi was 9.0% (range of 0%–27.0%), and the mean number of iRBCs per field was 100.7 (range 0.07–1000; Supplemental Table S2). As expected, control placentas did not contain hemozoin or iRBCs.

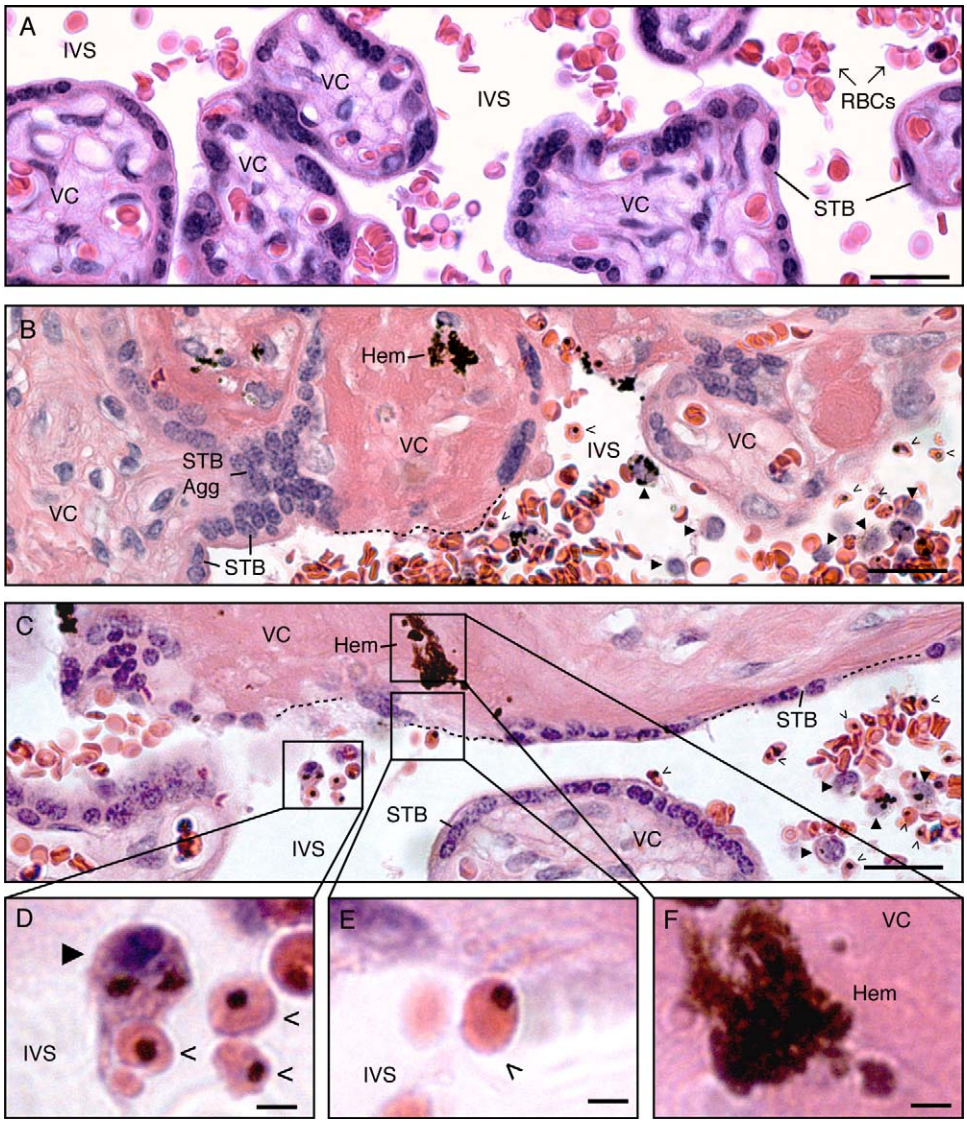

FIG. 1. STB loss is a prominent histopathological feature of placental malaria. **A**) In control, uninfected placentas, the villous core (VC), which contains stromal cells and fetal blood vessels, is covered by a continuous layer of STB. Maternal blood cells, primarily RBCs, occupy the intervillous space (IVS). **B**, **C**) In *P. falciparum*-infected placentas, STB denudation (dotted lines) brought the VC into direct contact with the IVS. Some denuded villi were acellular and eosinophilic (intravillous fibrinoid; **B**). Some exposed VCs resembled normal stroma (**C**). STB aggregation (STB Agg) was commonly observed. Villi that displayed these pathological alterations often contained hemozoin (Hem). These regions were reservoirs for iRBCs (open arrowheads) and maternal leukocytes (closed arrowheads). **D**) Cells with the morphological appearance of monocytes (closed arrowhead) contained hemozoin and were found in close association with iRBCs (open arrowheads). Infected RBCs (**E**) were observed adjacent to the VCs of denuded villi (**F**), which often contained hemozoin. Tissue sections were stained with H&E. Bars = 50 μm (**A**–**C**) and 10 μm (**D**–**F**).

We used linear regression analysis to investigate the relationship between STB denudation and markers of infection and inflammation. In the malaria group, STB denudation was positively associated with hemozoin-containing villi (regression coefficient [β] = 3% increase in denuded villi with each 5% increase in hemozoin-containing villi; SEM = 1%, P = 0.01; Fig. 2C) and the presence of maternal leukocytes (β = 2.1% increase in denuded villi for every 10 leukocytes; SEM = 0.5%, $P = 0.001$; Fig. 2D). No relationship was observed with iRBC frequency ($P = 0.88$; Fig. 2E). When we categorized the samples according to the well-established grading scheme developed by Bulmer et al. [38], STB denudation was more frequently observed in samples that contained hemozoin and were classed as either active-chronic or past-chronic infection (Supplemental Fig. S2). These data suggested that STB denudation was a feature of placentas categorized as having chronic malaria infection, as indicated by the presence of hemozoin.

Placental CD36 and ICAM1 Expression in Relationship to Maternal Blood Flow During Normal Pregnancy

We analyzed the expression patterns of the well-studied microvasculature receptors, CD36 and ICAM1, in healthy human placental biopsies (first trimester, second trimester, and term). We immunolocalized these receptors in cells that might mediate cytoadhesion: STB that cover the floating chorionic villi (Supplemental Fig. S1D, site 1) and endovascular iCTBs that line uterine blood vessels (Supplemental Fig. S1D, site 2). Isotype control Abs were used to monitor binding via fetal Fc receptors and did not react with any of the samples (Supplemental Fig. S4A). In floating chorionic villi (Fig.

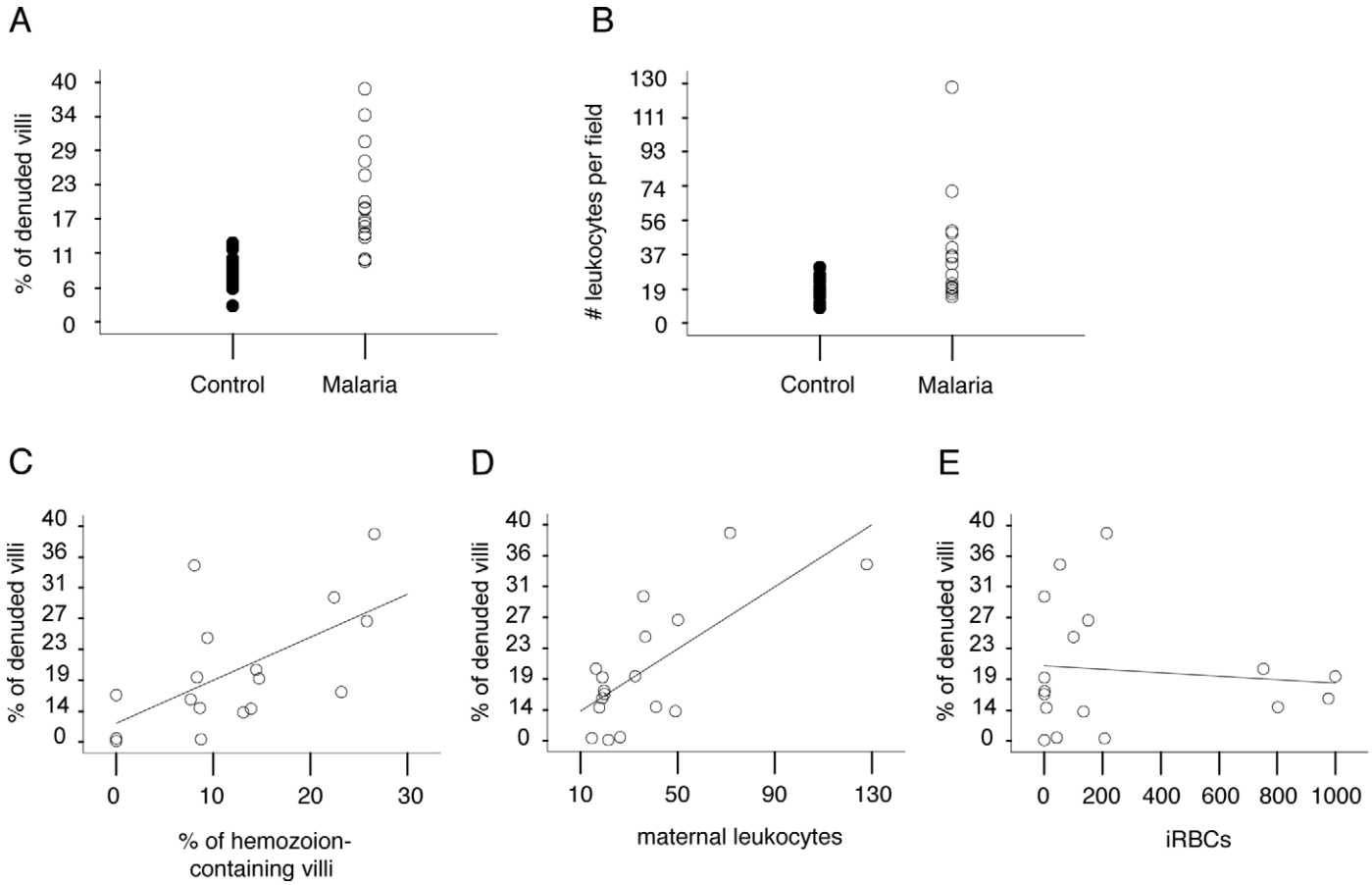

FIG. 2. STB denudation was associated with hemozoin and maternal leukocytes. **A**) STB denudation (# of denuded villi per total villi) was approximately two-fold higher in the cases versus controls (SEM = 2.2%, $P < 0.0001$). The mean percentage of STB loss was 9.0% in controls (closed circles; range 3.0%–13.0%) and 17.0% in the malaria group (open circles; range 10.0% to 39.0%). **B**) Maternal leukocyte infiltration was 18% higher in the cases versus controls (SEM = 7.0%, $P = 0.01$). The mean number of maternal leukocytes per 400× field was 18.0 in the controls (closed circles; range 8.6–30.5) and 26.3 in the malaria group (open circles; range 14.6–128.0). **C**–**E**) Linear regression analysis was used to determine associations between STB denudation and infection or inflammation. STB loss was associated with hemozoin (**C**; $P = 0.01$) and maternal leukocytes (**D**; $P = 0.001$), but not with iRBCs (**E**; $P = 0.88$).

3A), regardless of gestational age, CD36 staining (top panels) was observed in fetal blood vessels and the villous stromal core (green), but not in STB or underlying progenitor cytotrophoblasts (pCTBs). ICAM1 immunoreactivity (bottom panels) was not detected in first-trimester chorionic villi, but was identified in fetal blood vessels of second-trimester and term samples (green). STB and pCTBs did not stain.

We also analyzed second-trimester basal plate biopsies that contained iCTB-remodeled uterine arterioles (Fig. 3B). Invasive CTB invasion of uterine arterioles begins in the first trimester, peaks in the second trimester, and regresses at term. Accordingly, our studies focused on midgestation. In all samples, anti-CD36 and anti-ICAM1 mAbs reacted with the uterine extracellular matrix (green). Although iCTBs in the basal plate failed to express CD36, ICAM1 was detected on iCTBs that lined the uterine vessels (bottom panel, green). Similar staining patterns were observed at term (data not shown). Together, these results suggested that CD36 and ICAM1 are not normally in contact with the intervillous space. Endovascular iCTBs, however, which are in direct contact with maternal blood, expressed ICAM1, a known receptor for iRBCs.

Placental CS-A Expression in Relationship to Maternal Blood Flow During Normal Pregnancy

Given that CS-A is usually present in a heterogeneous mixture of CS-GAGs (see Supplemental Fig. S3 for details), we immunolocalized a broad array of these structures in floating chorionic villi (first-trimester, second-trimester and term). First, we employed mAbs that recognize epitopes containing CS-A: CS-56, LY111, and 473HD (Fig. 4A, upper half; mAb specificities are described in Supplemental Fig. S3) [49–52]. These mAbs strongly reacted with fetal blood vessels and/or the stromal villous cores (green); however, STB and underlying pCTBs did not stain. Anti-CS phage display Abs [50] had a similar pattern of reactivity (data not shown). All Abs failed to react with sections that were pretreated with chondroitinase ABC to remove CS-A (Supplemental Fig. S4B). Then, we immunolocalized unsaturated disaccharide isomers (ΔDi) created by chondroitinase ABC digestion of CS/dermatan sulfate (DS) proteoglycans (i.e., stubs). For this purpose, we used three mAbs: 2-B-6 (anti-proteoglycan ΔDi-4S), 3-B-3 (anti-proteoglycan ΔDi-6S), and 1-B-5 (anti-proteoglycan ΔDi-0S) [53, 54] (Fig. 4A, lower half; mAb specificities are described in Supplemental Fig. S3). These mAbs, including 2-B-6 that specifically recognizes epitopes derived from digestion of CS-A, reacted strongly with fetal

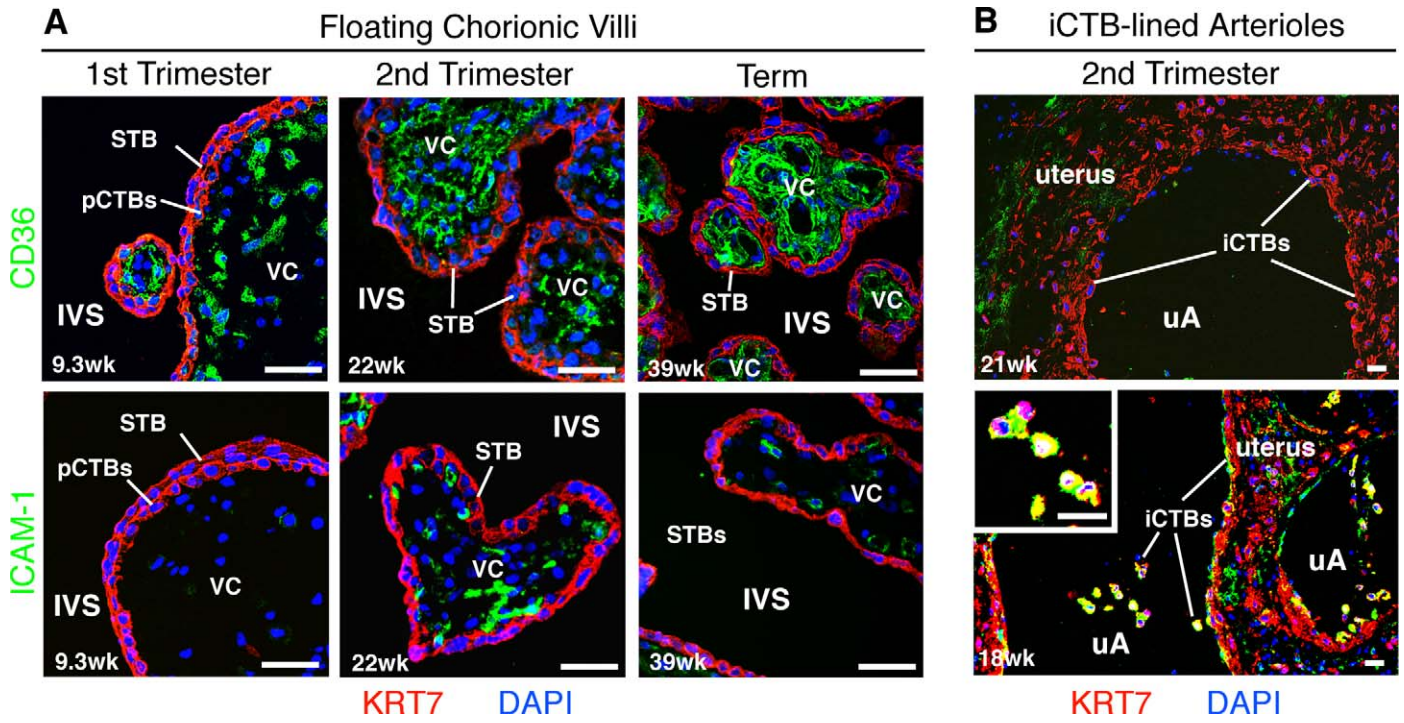

FIG. 3. CD36 and ICAM1 expression in relationship to the intervillous space during normal pregnancy. Tissue sections of placental biopsies from uncomplicated pregnancies (first-trimester, second-trimester, and term), corresponding to site 1 (**A**) and site 2 (**B**) in Supplemental Figure S1D, were analyzed. **A**) In floating chorionic villi at all gestational ages, anti-CD36 Ab (green, top panels) reacted with the stromal villous cores (VCs); pCTBs and STB failed to stain. ICAM1 expression (green, bottom panels), which was more variable, was not detected in first-trimester samples. Patchy staining of the VCs was evident beginning in the second trimester. No staining of the trophoblast layers was observed. **B**) Invasive CTB invasion of uterine arterioles (uAs) peaks in the second trimester. Therefore, these analyses focused on three placental samples that were collected from this time period. In basal plate biopsies that contained iCTB-remodeled uAs, anti-CD36 Ab (top panel) and anti-ICAM1 Ab (bottom panel) reacted with the uterine extracellular matrix (green). Invasive CTBs that lined the uAs failed to express CD36 (top panel), but stained brightly for ICAM1 (bottom panel), enlarged in inset. Biopsies were fixed in paraformaldehyde and frozen. STB and pCTBs were visualized by staining for cytokeratin 7 (KRT7, red). Nuclei were labeled with DAPI (blue). Bar = 40 μm.

blood vessels and/or the stromal villous core (green). Undigested (i.e., minus chondroitinase ABC) samples did not stain (Fig. 4A, lower half, insets). STB and pCTBs were not immunoreactive. These data showed that the stromal villous cores expressed CS-A, while STB and underlying pCTBs did not.

Finally, we analyzed second-trimester basal plate biopsies that contained iCTB-remodeled uterine arterioles (Fig. 4B). In all samples, the CS mAb panel reacted strongly with the uterine extracellular matrix (green), but failed to stain endovascular iCTBs that lined the uterine vessels. Together, these results suggested that CS-A, which is expressed among a heterogeneous mixture of CS-GAGs, is not in contact with maternal blood flow during normal pregnancy.

Placental CD36, ICAM1, and CS-A Expression in Relationship to Maternal Blood Flow During Malaria Infection

We determined the expression patterns of CD36, ICAM1, and CS-A in malaria-infected placentas collected from term deliveries in Kinshasa. Samples obtained from uninfected African women had the same staining patterns for the molecules of interest as shown for the healthy term placentas collected in San Francisco (data not shown). In infected samples, analysis of the chorionic villi (Fig. 5A) revealed that CD36 was expressed in the villous core. Due to STB denudation, immunopositive stromal areas were often in direct contact with maternal blood in the intervillous space. Staining for ICAM1 was primarily detected in association with fetal blood vessels in villous cores, with only minimal/patchy staining in the STB (Fig. 5A). Monoclonal Abs that reacted with CS-A (example shown for CS-56) showed staining throughout the villous core (within stroma or intravillous fibrinoid), which in some areas was continuous with the intervillous space (Fig. 5A, CS-56 inset). We attempted to stain these formalin-fixed, paraffin-embedded biopsies with the 2-B-6 stub mAb, but were unable to obtain a clear pattern of immunoreactivity due to nonspecific reactivity with undigested negative control samples (i.e., in the absence of chondroitinase ABC treatment).

Then, we analyzed term basal plate biopsies that contained iCTB-remodeled uterine arterioles (Fig. 5B). As shown for control samples collected in San Francisco (Fig. 3B), iCTBs that lined the arterioles expressed ICAM1. In this same location, CD36 and CS-A immunoreactivity were not detected (data not shown). Isotype control Abs, used to monitor binding via fetal Fc receptors, did not react with the samples (Supplemental Fig. S4C). Together, these findings suggested that malaria infection was associated with placental changes at a cellular level that brought known iRBC receptors on embryonic/fetal cells in direct contact with maternal blood.

Next, we examined the antigenic repertoire of maternal cells that come in contact with the placenta. First, we analyzed maternal leukocytes in the intervillous space (Fig. 5C). Cells with a morphological appearance of monocytes, which were adjacent to the placental surface or free floating in the intervillous space, stained for CD36 (upper panel) and ICAM1

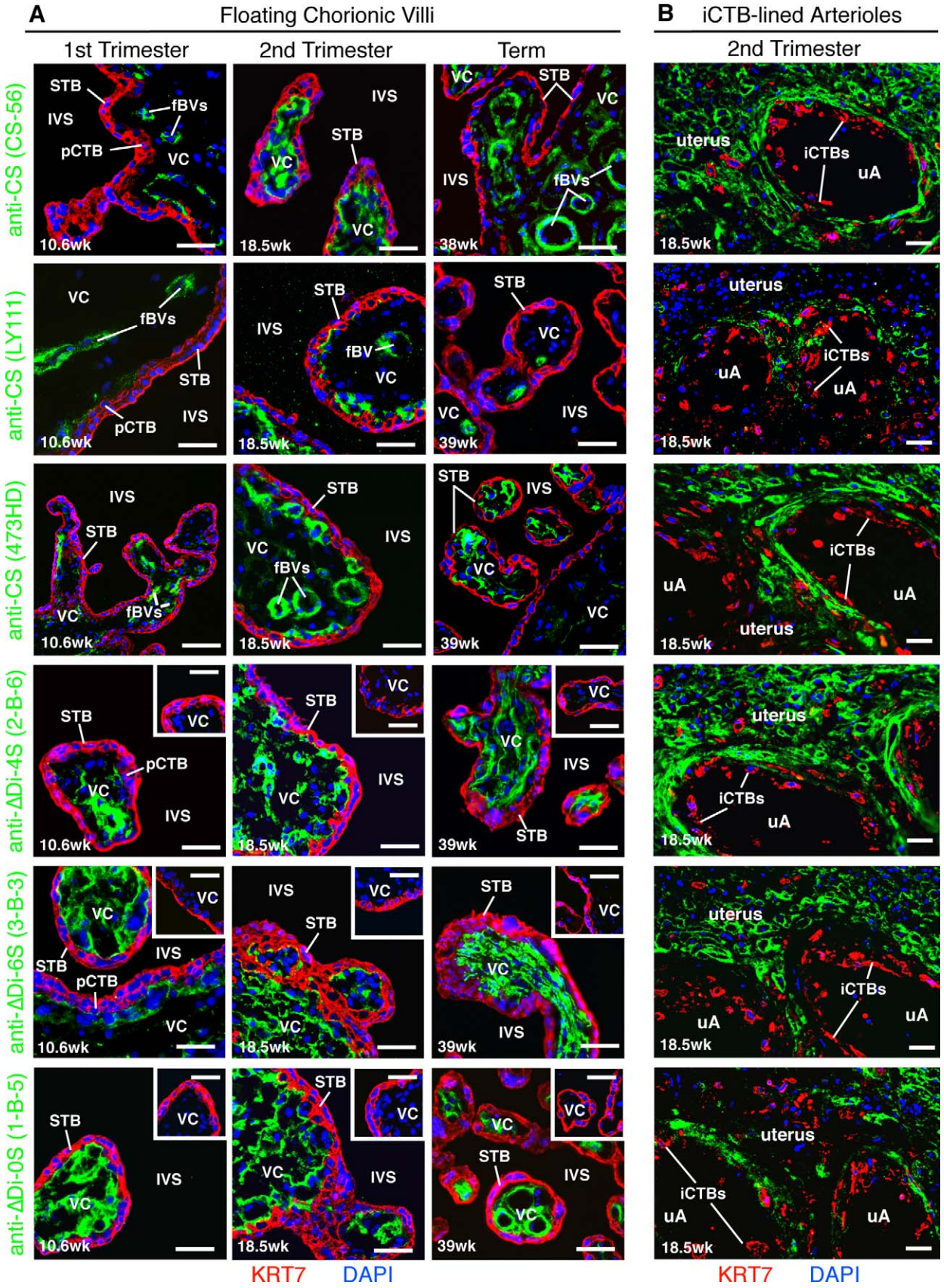

FIG. 4. CS-A expression is sequestered from the intervillous space during normal pregnancy. Biopsies from two placental sites (Supplemental Fig. S1D) were analyzed using the experimental strategy described in Figure 3. **A**) In floating chorionic villi, mAbs that specifically recognized CS-A (CS-56, LY111, 473HD) reacted with the villous cores (VCs) (green). Often, intense immunostaining was observed in association with fetal blood vessels (fBVs). The stub mAbs (2-B-6, 3-B-3, 1-B-5), which recognized epitopes exposed by chondroitinase ABC digestion, also reacted with the VCs (green). Control tissue sections that were not digested with chondroitinase ABC did not stain (insets). None of the mAbs stained STB or pCTBs, labeled with an anti-KRT7 mAb

(lower panel). CD36 is normally expressed by monocytes in other locations [55], and ICAM1 immunostaining has been detected in the setting of malaria [56]. In many cases, maternal leukocytes appeared to bridge iRBC adherence to the placenta. Staining for the known receptors was also observed in association with the portion of the uterus that lines the intervillous space (Fig. 5D). In the context of malaria, CD36 immunoreactivity was often associated with acellular regions (top panel). In contrast, ICAM1 expression was often cellular (bottom panel). Although CS-A was localized in the deeper uterine regions, maternal cells at the boundary with maternal blood failed to express this receptor (data not shown). In addition, placental septa, folds of the basal plate that project into intervillous space, also exhibited immunoreactivity (Fig. 5E). In these regions, staining for CD36 and ICAM1 was similar to that detected in association with the uterine surface (data not shown). Two mAbs that reacted with CS-A (CS-56 and LY111) showed widespread staining throughout the septal stroma, which in some cases was continuous with the intervillous space where iRBCs were found. In all locations, fibrin deposits occasionally stained for CD36, which could be a product of maternal platelets (data not shown) [57]. In every instance, isotype control Abs failed to react (Supplemental Fig. S4C). Together, these data demonstrated that maternal leukocytes at the placental surface and uterine cells that line the intervillous space expressed known receptors.

A Glycan Binding Screen Suggested a Role for Lewis Antigens in Cytoadhesion

We carried out a binding screen that utilized glycan arrays to explore novel receptors that might mediate adhesion. Previously, this approach was used to identify ligands/receptors involved in pathogen adherence to host cells [58]. We focused on carbohydrate structures because the placenta expresses an unusual repertoire of glycans and modulates glycosylation as a function of gestational age [59]. We bound fluorescently labeled iRBCs to printed slides displaying 377 natural and synthetic glycan motifs [45, 46]. These arrays present numerous structural motifs that are recognized by glycan-binding proteins, but do not include CS-GAGs that contain the CS-A motif. We used the *P. falciparum* CS2 line that was generated by panning on Chinese hamster ovary cells and purified CS-A [60] and is often used to study iRBC adherence in vitro. The results from two independent experiments are summarized in an annotated heat map of potential binding partners (Fig. 6A), and the oligosaccharide structures are included in Supplemental Figure S6. Infected RBCs adhered to saccharides that carry a subset of Lewis (Le) blood group structures—(s)Le^x, Le^y, Le^b—sialyl N-acetyllactosamine (LacNAc), sulfated derivatives of LacNAc and Le^x, and the blood group A antigen. These results suggested that iRBCs can bind core motifs that are common in glycan structures (e.g., LacNAc) and specialized termini including Le antigens and sulfate-containing carbohydrate substituents.

Immunoblotting and Immunostaining Revealed that Lewis Antigens Are Positioned to Support Cytoadhesion

We used an immunoblotting approach to determine whether STB expressed the motifs that iRBCs bound on the arrays. These experiments utilized STB microvillous membrane fractions that were prepared from placentas of different gestational ages collected in San Francisco. Figure 6B shows the high-molecular-weight regions of the blots where most of the specific immunoreactivity was detected. Preparations from 6- and 9-wk placentas had appreciable levels of Le^x expression that were apportioned among several glycoproteins (Fig. 6B, top, left). Ab reactivity appeared to decline with advancing gestational age. sLe^x expression was limited to a subset of high-molecular-weight species that also appeared to be more abundant during early gestation (Fig. 6B, top, middle). The HECA-452 Ab, which recognizes sLe^x and 6-sulfo sLe^x (the sulfate is permissive, but not required for reactivity) [61], had a similar pattern of expression (Fig. 6B, top, right). In contrast, the MECA-79 Ab, which binds related glycans including 6-sulfo LacNAc, did not react with STB preparations (data not shown). Expression of the other Le antigens we assayed is determined by a complex system of genetic regulation that leads to individual differences [62]. Le^a expression was not detected (Fig. 6B, bottom, left). Le^y (Fig. 6B, bottom, middle) expression was observed in most samples collected during the first half of pregnancy, while Le^b (Fig. 6B, bottom, right) immunoreactivity was primarily confined to a 9-wk preparation.

We also immunostained tissue sections of first-trimester floating chorionic villi (collected in San Francisco) with mAbs that recognized the Le antigens that were detected by immunoblotting (Fig. 6C). No expression of Le^y or Le^b was observed (data not shown), which may be explained by genetic variation. Patchy Le^x (top panel) and sLe^x (middle panel) expression was detected in association with STB. The HECA-452 mAb, which recognizes sLe^x and 6-sulfo sLe^x [61], also stained STB (lower panel). As predicted from the immunoblotting data that spanned a wide range of gestational ages (Fig. 6B), no (s)Le^x immunoreactivity was visualized in malaria-infected placentas at term (Fig. 6D). In contrast, Le^x (Fig. 6D, top panel) and sLe^x (Fig. 6D, bottom panel) were expressed by cells with the morphological appearance of maternal monocytes to which iRBCs appeared to cytoadhere. HECA-452 immunoreactivity was not detected. These results demonstrated that STB expressed sulfated and unsulfated (s)Le^x glycan motifs in early gestation and suggested that these structures are positioned to initiate cytoadhesion in the absence of malaria-related pathologies. At later stages of infection, leukocyte-associated (s)Le^x motifs may also bind iRBCs.

DISCUSSION

STB denudation, which is normally uncommon, was first described in *P. falciparum*-infected human placentas over thirty years ago [9, 32] and more recently documented by Crocker et al. [39]. Here we show, for the first time, a detailed histopathological analysis of the STB layer of infected placentas in the context of control samples. Specifically, we quantified STB denudation, and our results suggest that it could influence cytoadhesion. STB loss was approximately two-fold higher in *P. falciparum*-infected placentas; in extreme cases, 39% of the villi exhibited this lesion. STB denudation appeared to be a feature of chronic infection, as it correlated with hemozoin deposition and increased numbers of maternal leukocytes. Intriguingly, STB loss appeared to expose known

(red). **B**) In second-trimester basal plate biopsies that contained iCTB-remodeled uterine arterioles (uAs), the anti-CS-A mAb panel reacted with the uterine extracellular matrix, but failed to stain iCTBs that lined the uAs. Bar = 40 μm.

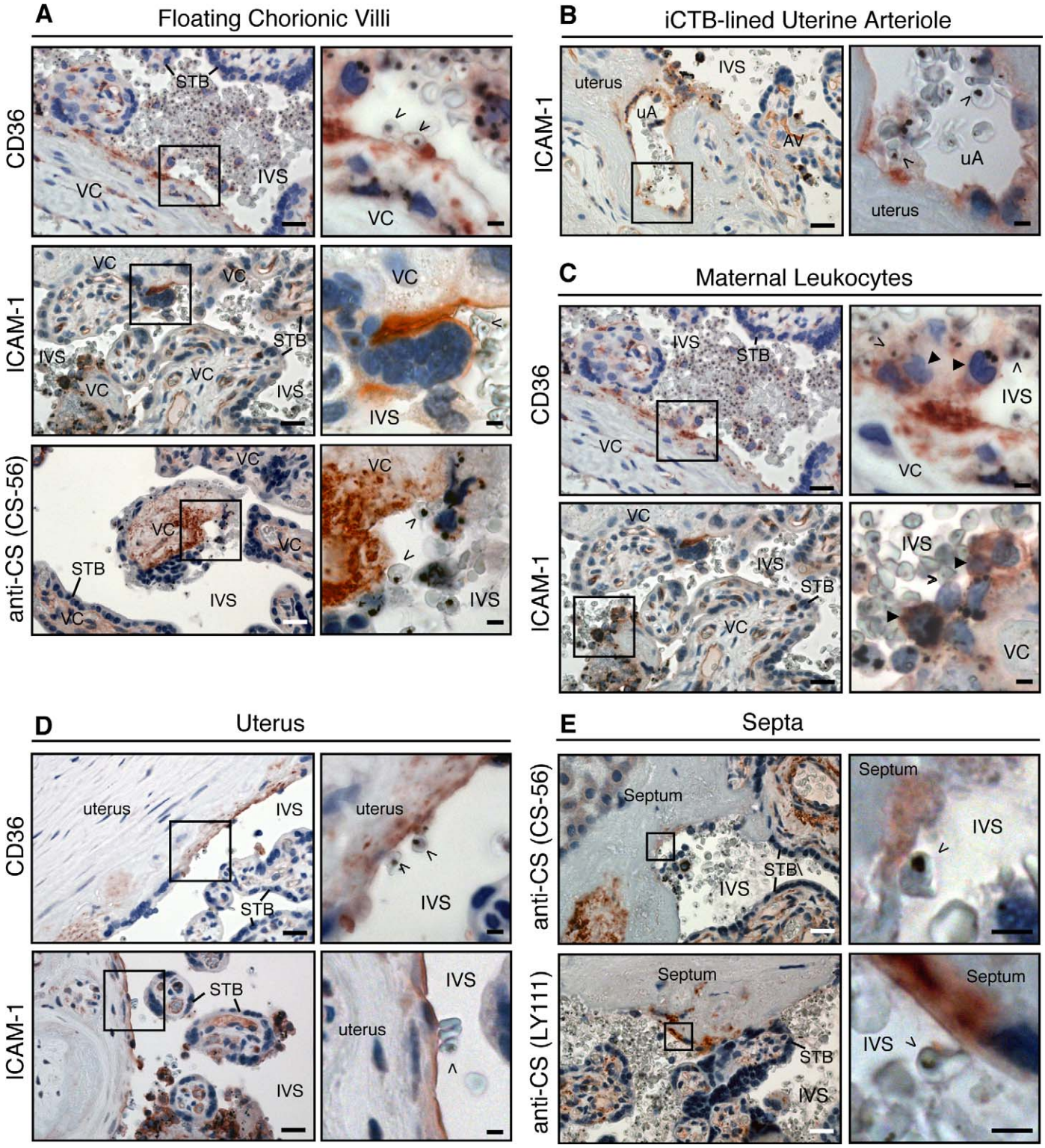

FIG. 5. CD36, ICAM1, and CS-A expression in relationship to the intervillous space during malaria infection. **A**) In floating chorionic villi, villous core (VC) regions that were denuded of STB expressed CD36. STB exhibited patchy ICAM1 immunoreactivity. Abs that recognized CS-A (example shown for CS56) reacted with denuded regions (inset) and intact stroma. **B**) As shown for normal samples collected in San Francisco (Fig. 3B), iCTBs that lined uterine arterioles (uAs) expressed ICAM1. Anchoring villus, AV. **C**) Maternal leukocytes in the intervillous space (IVS) with the morphological appearance of monocytes (closed arrowheads) stained for CD36 (top panel) and ICAM1 (bottom panel). Often, these cells formed a bridge between iRBCs (open arrowheads) and STB. **D**) The portion of the uterus that lines the intervillous space expressed CD36 (top panel) and ICAM1 (bottom panel). **E**) Placental septa (Supplemental Fig. S1B) that were continuous with the intervillous space stained for CS-A (detected with CS-56 and LY111 mAbs). The brown color represents the binding of primary Abs. Sections were counterstained with hematoxylin (blue). Boxed area in left panel is enlarged as right panel. Bars = 50 μm for lower magnification and 10 μm for higher magnification micrographs.

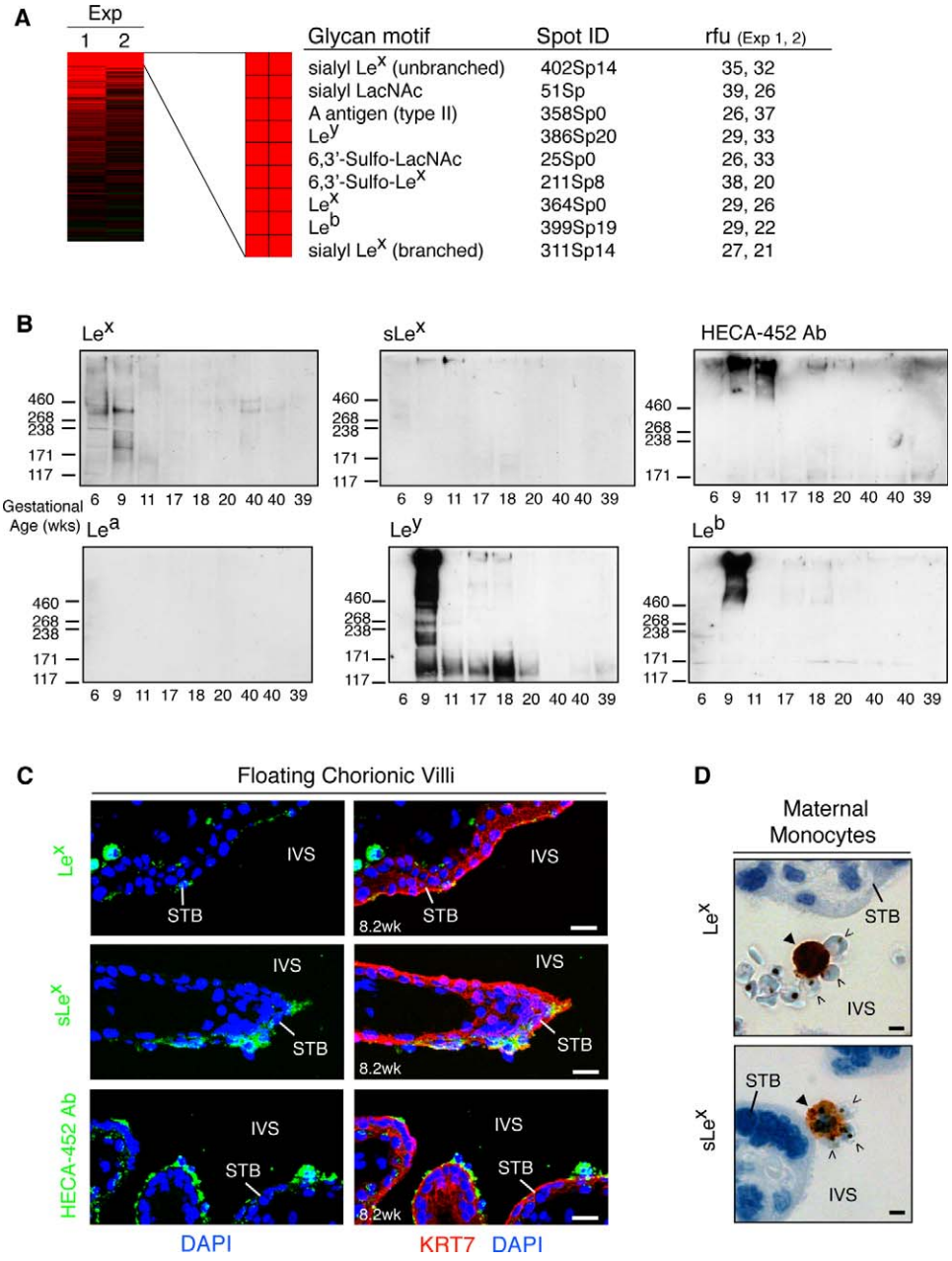

FIG. 6. A glycan binding screen suggests a role for Le carbohydrate antigens in cytoadhesion. **A**) Fluorescently labeled iRBCs were bound to a glycan array. An annotated heat map of potential *P. falciparum* binding partners that were detected in both experiments (Exp 1 2) is shown. These included a preponderance of Le blood group structures. Relative fluorescent units (rfu) were computed as the foreground minus background intensity. **B**) STB microvillous membranes were isolated from placentas of the gestational ages shown, separated by SDS-PAGE, and probed with mAbs that recognized the glycans that iRBCs bound on the arrays. The apparent molecular masses of markers (shown as $M_r \times 10^{-3}$) are on the left. First-trimester placentas had appreciable levels of Le^x, sLe^x, and sulfated Le^x (detected with HECA-452 Ab) expression (top blots). Ab reactivity declined with advancing gestational age. In contrast, Le^a expression was not detected (bottom, left). Le^y (bottom, middle) immunoreactivity was observed in most samples collected during the first half of pregnancy, while Le^b (bottom, right) expression was primarily confined to a 9-wk preparation. **C**) First-trimester placental biopsies from uncomplicated pregnancies were fixed in paraformaldehyde and frozen. In floating chorionic villi, STB exhibited patchy Le^x (top panel) and sLe^x (middle panel) expression (green). STB uniformly stained for sulfated sLe^x (green, bottom panel). Bar = 20 μm. **D**) *P. falciparum*-infected, term placentas were formalin fixed and paraffin embedded. Maternal leukocytes with the morphological appearance of monocytes (closed arrowheads) expressed Le^x (top panel) and sLe^x (bottom panel). Infected RBCs (open arrowheads) were found in close association with these cells. Bar = 40 μm.

receptors to maternal blood. Immunolocalization of CD36 and CS-A revealed that they were abundantly expressed in the villous stromal core, a location that is not normally in contact with the intervillous space. Upon STB denudation, however, CD36 and CS-A were in direct contact with iRBC-containing maternal blood. Although we do not know why *P. falciparum*-infected placentas display this lesion, it has been noted in other pregnancy complications [41, 63], and there is evidence that inflammation may be a cause. For example, in vitro experiments demonstrated that monocyte adhesion to syncytium and concomitant production of tissue necrosis factor alpha (TNF-α) promoted STB loss [64]. Since increased levels of TNF-α are associated with placental malaria [65] and have been noted by other groups in association with cytomegalovirus infection of the placenta [66, 67], this mechanism may

account for the loss of syncytial integrity that we observed in our samples.

Intriguingly, our results suggest that CS-A, the best-described placental receptor, is not expressed by the STB microvillous surface that is thought to initiate sequestration. Infected RBCs isolated from term placental blood bind this glycan in vitro [16, 17], and Ricke et al. [21] showed that Abs from malaria-exposed pregnant women can block this interaction. In this context, our results suggest that STB denudation brought placental CS-A in contact with iRBC-containing maternal blood. We employed a panel of mAbs to localize CS-A. In all samples (n = 18), regardless of infection status or tissue-processing technique (paraformaldehyde fixed, frozen versus formalin fixed, paraffin embedded), the villous core expressed CS-A, while STB, iCTBs, and the intervillous space did not. Our conclusions vary from previously published reports [30, 68–70]. The reasons may include methodological differences (immunolocalization versus biochemical fractionation). Achur et al. [70] purified CS proteoglycans from human placentas by enriching for uronic acid-containing glycans and then depleting hyaluronan and heparan sulfate GAGs with glycosidases. In agreement with our data, the majority (74%) were in the fibrous (i.e., stromal) cores. In contrast, they concluded that the remaining CS-GAGs were STB associated (2%) or free floating in the intervillous space (24%). We speculate that incomplete glycosidase treatment and/or uterine, stromal, or blood contamination of these fractions could account for the latter findings.

In a few cases, immunolocalization of CS-A in placental sections has been described [68, 69, 71]. These results, however, are not directly comparable to ours because, for the most part, we employed different Abs. Our group used mAbs that recognize CS-A among a heterogeneous mixture of CS-GAGs (CS-56, LY111, 473HD), while Muthusamy et al. [68, 69] used pAbs that, to our knowledge, recognize undefined epitopes. In one instance, we used the same 2-B-6 stub mAb (anti-proteoglycan ΔDi-4S), but obtained different results, which may be attributable to alternative techniques. In the previous study, tissue processing was accomplished by microwaving samples in fixing medium prior to embedding; this was done to preserve material in the intervillous space [69]. Another difference is that we employed a more stringent blocking protocol, controlling for nonspecific binding to both unoccupied (with serum) and occupied (with anti-human IgG) Fc receptors. In our experience, unambiguous detection of placental antigens is complicated by ex vivo fibrin deposition that results from suboptimal tissue handling, STB expression of fetal Fc receptors [72, 73], and abundant endogenous peroxidase activity, all of which must be controlled for to prevent nonspecific reactivity.

Our results also showed that a variety of cells at the maternal-fetal interface express CD36 and/or ICAM1. Endovascular iCTBs, which line uterine arterioles that channel maternal blood flow to the placenta, expressed ICAM1 regardless of infection status. This finding agreed with a previous report [29]. Therefore, these cells are positioned to mediate cytoadhesion via this or other iRBC receptors that they express: VCAM-1, PECAM, and NCAM-1 [74–76]. In many instances, potential cytoadhesion mechanisms were only apparent when we analyzed infected samples. In agreement with previous studies [10, 28], we found that malaria is associated with patchy STB ICAM1 expression, which in other settings is induced by interleukin-1 (IL-1) and TNF-α. Interestingly, our results suggested that perivillous maternal leukocytes may contribute to the retention of parasites at the surface of the placenta. We observed iRBCs in close

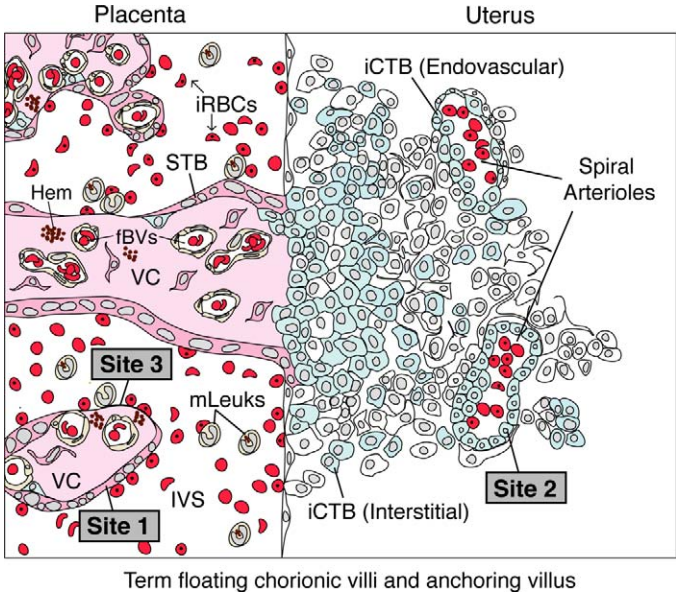

FIG. 7. A model for *P. falciparum* sequestration by the human placenta. At a microanatomical level, *P. falciparum* infection changes the repertoire of placental tissues that are in direct contact with maternal blood. In this context, binding to STB (site 1) and/or iCTBs that line uterine vessels (site 2) initiates sequestration. At later stages, STB denudation brings site 3, the villous core (VC), into direct contact with maternal blood. At a molecular level, sequestration might be initiated when iRBCs adhere to STB via currently unidentified molecules and/or to endovascular iCTBs that line uterine arterioles and express ICAM1 (site 2). As infection progresses, cytoadherence to STB might also occur via ICAM1. Advanced stages of placental malaria are associated with hemozoin (Hem) and STB denudation, which exposes villous CD36 and CS-A to maternal blood (site 3). Placenta-associated maternal leukocytes (mLeuk) could also participate in adherence because they express CD36, ICAM1, and Le antigens.

relationship to maternal leukocytes that expressed known monocyte markers (ICAM1 and CD36 [55, 56]), and in many instances monocytes also bound STB, appearing to bridge iRBCs and the syncytium.

Together, our findings suggest that CS-A, CD36, and ICAM1 are primarily positioned to mediate cytoadhesion in advanced and/or chronic infection that correlates with leukocyte infiltration and STB denudation. This implies that, at the onset of infection, as-yet-unidentified molecules facilitate binding to the intact syncytium and/or iCTBs. In this regard, during the first trimester, blood slowly percolates in the nascent intervillous space, and placental iCTBs begin to invade the uterine vasculature [6]. By the beginning of the second trimester, remodeling of the uterine arterioles establishes robust blood flow to the placenta. Here, we demonstrated that Le antigens ([s]Le^x, Le^y, and Le^b), which bound iRBCs, are positioned to promote placental cytoadhesion. Interestingly, STB expressed (s)Le^x and related sulfated glycans in the first trimester and down-regulated their expression with advancing gestational age. Endovascular iCTBs that line the uterine arterioles, also expressed sLe^x [77]. Le^y and Le^b were detected on STB to varying degrees in some samples, but were absent in others. Finally, other data implicate additional terminal saccharides in initial adhesion. Glycans containing alpha 2-6-linked sialic acid are expressed at high levels on the STB microvillous surface of malaria-infected placentas [78] where they could facilitate the first steps of infection. In this regard, we detected iRBC binding to an alpha 2-6-containing saccharide on the glycan array. Thus, we and others provide

evidence that Le antigens and other sialic acid-containing oligosaccharides could play a role in iRBC adhesion to the placental surface. It will be interesting to determine, in the future, whether similar or different carbohydrate binding specificities are displayed by other *P. falciparum* lines.

In summary, this work contributes to our understanding of iRBC sequestration by the placenta. The results showed that both placental and maternal cells are positioned to promote cytoadhesion (Fig. 7) and that their roles may vary at different stages of infection. In this regard, a novel glycan binding screen identified new candidate receptors for iRBCs, and we showed that a subset is expressed at the placental surface during the beginning of pregnancy. Thus, Le carbohydrate antigens could play an important role in the initial steps of placental malaria. Our work also gave insights into the molecular mechanisms that are involved in the later stages. Specifically, the data presented here suggest that sequestration is influenced by STB denudation, which exposes previously masked receptors to the intervillous space. As to the molecules involved, our work clarified the localization pattern of CS-A and demonstrated that CD36 and ICAM1 are exposed to maternal blood in the setting of infection. Thus, we suggest that the step-wise mechanisms that mediate iRBC adhesion to chorionic villi should be revisited if preventing initial adhesion is the goal of therapeutic interventions.

ACKNOWLEDGMENT

We are grateful to the women who participated in this study. We are indebted to Dr. Linda Wright for facilitating the collaboration with our Congolese colleagues. We thank Dr. Mirhan Kapidzic, Mr. Jake Scott, Ms. Haley Stolp, and Mr. Gabriel Goldfien for excellent assistance in collecting placentas in San Francisco. We are grateful to Ms. Linda Prentice for tissue processing, Dr. Grace Kim for expertise on placental pathologies, Dr. Jacqueline Gilmore for biopsy scoring, Dr. Matthew Miller for support with *P. falciparum* cultures, and Mr. Matthew Donne for assistance with confocal microscopy. We thank Dr. Andreas Faissner for gifting the 473HD mAb, Dr. Toin van Kuppevelt for the phage display Abs, and MR4 for providing the *P. falciparum* line CS2. We are indebted to Drs. David Smith and Jamie Heimburg-Molinaro with the Consortium for Functional Glycomics for providing glycan arrays and technical advice. We thank Drs. Kurt Benirschke, Philip Rosenthal, Alicia Barcena, Steven Rosen, and Michael McMaster for careful reading of this manuscript.

REFERENCES

1. Desai M, ter Kuile FO, Nosten F, McGready R, Asamoa K, Brabin B, Newman RD. Epidemiology and burden of malaria in pregnancy. Lancet Infect Dis 2007; 7:93–104.
2. Rogerson SJ, Mwapasa V, Meshnick SR. Malaria in pregnancy: linking immunity and pathogenesis to prevention. Am J Trop Med Hyg 2007; 77: 14–22.
3. Rogerson SJ, Hviid L, Duffy PE, Leke RF, Taylor DW. Malaria in pregnancy: pathogenesis and immunity. Lancet Infect Dis 2007; 7: 105–117.
4. Brabin BJ, Romagosa C, Abdelgalil S, Menendez C, Verhoeff FH, McGready R, Fletcher KA, Owens S, D'Alessandro U, Nosten F, Fischer PR, Ordi J. The sick placenta—the role of malaria. Placenta 2004; 25: 359–378.
5. Brabin B, Johnson P. Placental malaria and pre-eclampsia through the looking glass backwards? J Reprod Immunol 2005; 65:1–15.
6. Benirschke K, Kaufmann P, Baergen RN. Pathology of the Human Placenta. New York: Springer Science+Business Media, Inc; 2006.
7. Brabin BJ. An analysis of malaria in pregnancy in Africa. Bull World Health Organ 1983; 61:1005–1016.
8. Bray R, Sinden R. The sequestration of *Plasmodium falciparum* infected erythrocytes in the placenta. Trans R Soc Trop Med Hyg 1979; 73: 716–719.
9. Galbraith RM, Fox H, Hsi B, Galbraith GM, Bray RS, Faulk WP. The human materno-foetal relationship in malaria. II. Histological, ultrastructural and immunopathological studies of the placenta. Trans R Soc Trop Med Hyg 1980; 74:61–72.
10. Sugiyama T, Cuevas LE, Bailey W, Makunde R, Kawamura K, Kobayashi M, Masuda H, Hommel M. Expression of intercellular adhesion molecule 1 (ICAM-1) in *Plasmodium falciparum*-infected placenta. Placenta 2001; 22:573–579.
11. Baruch DI, Pasloske BL, Singh HB, Bi X, Ma XC, Feldman M, Taraschi TF, Howard RJ. Cloning the *P. falciparum* gene encoding PfEMP1, a malarial variant antigen and adherence receptor on the surface of parasitized human erythrocytes. Cell 1995; 82:77–87.
12. Hviid L, Salanti A. VAR2CSA and protective immunity against pregnancy-associated *Plasmodium falciparum* malaria. Parasitology 2007; 134:1871–1876.
13. Salanti A, Staalsoe T, Lavstsen T, Jensen AT, Sowa MP, Arnot DE, Hviid L, Theander TG. Selective upregulation of a single distinctly structured var gene in chondroitin sulphate A-adhering *Plasmodium falciparum* involved in pregnancy-associated malaria. Mol Microbiol 2003; 49:179–191.
14. Beeson JG, Rogerson SJ, Elliott SR, Duffy MF. Targets of protective antibodies to malaria during pregnancy. J Infect Dis 2005; 192: 1647–1650.
15. Brown A, Higgins MK. Carbohydrate binding molecules in malaria pathology. Curr Opin Struct Biol 2010; 20:560–566.
16. Fried M, Duffy P. Adherence of *Plasmodium falciparum* to chondroitin sulfate A in the human placenta. Science 1996; 272:1502–1504.
17. Beeson JG, Brown GV, Molyneux ME, Mhango C, Dzinjalamala F, Rogerson SJ. *Plasmodium falciparum* isolates from infected pregnant women and children are associated with distinct adhesive and antigenic properties. J Infect Dis 1999; 180:464–472.
18. Duffy M, Maier A, Byrne T, Marty A, Elliott S, O'Neill M, Payne P, Rogerson S, Cowman A, Crabb B, Brown G. VAR2CSA is the principal ligand for chondroitin sulfate A in two allogeneic isolates of *Plasmodium falciparum*. Mol Biochem Parasitol 2006; 148:117–124.
19. Viebig N, Gamain B, Scheidig C, Lepolard C, Przyborski J, Lanzer M, Gysin J, Scherf A. A single member of the *Plasmodium falciparum* var multigene family determines cytoadhesion to the placental receptor chondroitin sulphate A. EMBO Rep 2005; 6:775–781.
20. Salanti A, Dahlback M, Turner L, Nielsen MA, Barfod L, Magistrado P, Jensen AT, Lavstsen T, Ofori MF, Marsh K, Hviid L, Theander TG. Evidence for the involvement of VAR2CSA in pregnancy-associated malaria. J Exp Med 2004; 200:1197–1203.
21. Ricke CH, Staalsoe T, Koram K, Akanmori BD, Riley EM, Theander TG, Hviid L. Plasma antibodies from malaria-exposed pregnant women recognize variant surface antigens on *Plasmodium falciparum*-infected erythrocytes in a parity-dependent manner and block parasite adhesion to chondroitin sulfate A. J Immunol 2000; 165:3309–3316.
22. Flick K, Scholander C, Chen Q, Fernandez V, Pouvelle B, Gysin J, Wahlgren M. Role of nonimmune IgG bound to PfEMP1 in placental malaria. Science 2001; 293:2098–2100.
23. Rasti N, Namusoke F, Chene A, Chen Q, Staalsoe T, Klinkert M, Mirembe F, Kironde F, Wahlgren M. Nonimmune immunoglobulin binding and multiple adhesion characterize *Plasmodium falciparum*-infected erythrocytes of placental origin. Proc Natl Acad Sci U S A 2006; 103: 13795–13800.
24. Beeson J, Rogerson S, Cooke B, Reeder J, Chai W, Lawson A, Molyneux M, Brown G. Adhesion of *Plasmodium falciparum*-infected erythrocytes to hyaluronic acid in placental malaria. Nat Med 2000; 6:86–90.
25. Muthusamy A, Achur RN, Valiyaveettil M, Botti JJ, Taylor DW, Leke RF, Gowda DC. Chondroitin sulfate proteoglycan but not hyaluronic acid is the receptor for the adherence of *Plasmodium falciparum*-infected erythrocytes in human placenta, and infected red blood cell adherence up-regulates the receptor expression. Am J Pathol 2007; 170:1989–2000.
26. Turner GD, Morrison H, Jones M, Davis TM, Looareesuwan S, Buley ID, Gatter KC, Newbold CI, Pukritayakamee S, Nagachinta B, White NJ, Berendt AR. An immunohistochemical study of the pathology of fatal malaria. Evidence for widespread endothelial activation and a potential role for intercellular adhesion molecule-1 in cerebral sequestration. Am J Pathol 1994; 145:1057–1069.
27. Grau GE, Mackenzie CD, Carr RA, Redard M, Pizzolato G, Allasia C, Cataldo C, Taylor TE, Molyneux ME. Platelet accumulation in brain microvessels in fatal pediatric cerebral malaria. J Infect Dis 2003; 187: 461–466.
28. Sartelet H, Garraud O, Rogier C, Milko-Sartelet I, Kaboret Y, Michel G, Roussilhon C, Huerre M, Gaillard D. Hyperexpression of ICAM-1 and CD36 in placentas infected with *Plasmodium falciparum*: a possible role of these molecules in sequestration of infected red blood cells in placentas. Histopathology 2000; 36:62–68.
29. Burrows TD, King A, Loke YW. Expression of adhesion molecules by endovascular trophoblast and decidual endothelial cells: implications for vascular invasion during implantation. Placenta 1994; 15:21–33.

30. Maubert B, Guilbert LJ, Deloron P. Cytoadherence of *Plasmodium falciparum* to intercellular adhesion molecule 1 and chondroitin-4-sulfate expressed by the syncytiotrophoblast in the human placenta. Infect Immun 1997; 65:1251–1257.
31. Ordi J, Ismail MR, Ventura PJ, Kahigwa E, Hirt R, Cardesa A, Alonso PL, Menendez C. Massive chronic intervillositis of the placenta associated with malaria infection. Am J Surg Pathol 1998; 22:1006–1011.
32. Walter PR, Garin Y, Blot P. Placental pathologic changes in malaria. A histologic and ultrastructural study. Am J Pathol 1982; 109:330–342.
33. Yamada M, Steketee R, Abramowsky C, Kida M, Wirima J, Heymann D, Rabbege J, Breman J, Aikawa M. *Plasmodium falciparum* associated placental pathology: a light and electron microscopic and immunohistologic study. Am J Trop Med Hyg 1989; 41:161–168.
34. Ordi J, Menendez C, Ismail MR, Ventura PJ, Palacin A, Kahigwa E, Ferrer B, Cardesa A, Alonso PL. Placental malaria is associated with cell-mediated inflammatory responses with selective absence of natural killer cells. J Infect Dis 2001; 183:1100–1107.
35. Menendez C, Ordi J, Ismail MR, Ventura PJ, Aponte JJ, Kahigwa E, Font F, Alonso PL. The impact of placental malaria on gestational age and birth weight. J Infect Dis 2000; 181:1740–1745.
36. Rogerson SJ, Pollina E, Getachew A, Tadesse E, Lema VM, Molyneux ME. Placental monocyte infiltrates in response to *Plasmodium falciparum* malaria infection and their association with adverse pregnancy outcomes. Am J Trop Med Hyg 2003; 68:115–119.
37. Galbraith RM, Faulk WP, Galbraith GM, Holbrook TW, Bray RS. The human materno-foetal relationship in malaria: I. Identification of pigment and parasites in the placenta. Trans R Soc Trop Med Hyg 1980; 74:52–60.
38. Bulmer JN, Rasheed FN, Francis N, Morrison L, Greenwood BM. Placental malaria. I. Pathological classification. Histopathology 1993; 22: 211–218.
39. Crocker I, Tanner O, Myers J, Bulmer J, Walraven G, Baker P. Syncytiotrophoblast degradation and the pathophysiology of the malaria-infected placenta. Placenta 2004; 25:273–282.
40. Bulmer JN, Rasheed FN, Morrison L, Francis N, Greenwood BM. Placental malaria. II. A semi-quantitative investigation of the pathological features. Histopathology 1993; 22:219–225.
41. Zhou Y, Bianco K, Huang L, Nien J, McMaster M, Romero R, Fisher S. Comparative analysis of maternal-fetal interface in preeclampsia and preterm labor. Cell Tissue Res 2007; 329:559–569.
42. Damsky CH, Fitzgerald ML, Fisher SJ. Distribution patterns of extracellular matrix components and adhesion receptors are intricately modulated during first trimester cytotrophoblast differentiation along the invasive pathway, in vivo. J Clin Invest 1992; 89:210–222.
43. Romagosa C, Menendez C, Ismail MR, Quinto L, Ferrer B, Alonso PL, Ordi J. Polarisation microscopy increases the sensitivity of hemozoin and Plasmodium detection in the histological assessment of placental malaria. Acta Trop 2004; 90:277–284.
44. Lambros C, Vanderberg JP. Synchronization of *Plasmodium falciparum* erythrocytic stages in culture. J Parasitol 1979; 65:418–420.
45. Smith DF, Song X, Cummings RD. Use of glycan microarrays to explore specificity of glycan-binding proteins. Methods Enzymol 2010; 480: 417–444.
46. Heimburg-Molinaro J, Song X, Smith DF, Cummings RD. Preparation and analysis of glycan microarrays. Curr Protoc Protein Sci 2011; 64: 12.10.1–12.10.29.
47. Lawrence MB, Springer TA. Leukocytes roll on a selectin at physiologic flow rates: distinction from and prerequisite for adhesion through integrins. Cell 1991; 65:859–873.
48. Smith CH, Nelson DM, King BF, Donohue TM, Ruzycki S, Kelley LK. Characterization of a microvillous membrane preparation from human placental syncytiotrophoblast: a morphologic, biochemical, and physiologic study. Am J Obstet Gynecol 1977; 128:190–196.
49. Ito Y, Hikino M, Yajima Y, Mikami T, Sirko S, von Holst A, Faissner A, Fukui S, Sugahara K. Structural characterization of the epitopes of the monoclonal antibodies 473HD, CS-56, and MO-225 specific for chondroitin sulfate D-type using the oligosaccharide library. Glycobiology 2005; 15:593–603.
50. Smetsers TF, van de Westerlo EM, ten Dam GB, Overes IM, Schalkwijk J, van Muijen GN, van Kuppevelt TH. Human single-chain antibodies reactive with native chondroitin sulfate detect chondroitin sulfate alterations in melanoma and psoriasis. J Invest Dermatol 2004; 122: 707–716.
51. Deepa SS, Yamada S, Fukui S, Sugahara K. Structural determination of novel sulfated octasaccharides isolated from chondroitin sulfate of shark cartilage and their application for characterizing monoclonal antibody epitopes. Glycobiology 2007; 17:631–645.
52. Sugahara K, Mikami T. Chondroitin/dermatan sulfate in the central nervous system. Curr Opin Struct Biol 2007; 17:536–545.
53. Poole CA, Glant TT, Schofield JR. Chondrons from articular cartilage. (IV). Immunolocalization of proteoglycan epitopes in isolated canine tibial chondrons. J Histochem Cytochem 1991; 39:1175–1187.
54. Couchman JR, Caterson B, Christner JE, Baker JR. Mapping by monoclonal antibody detection of glycosaminoglycans in connective tissues. Nature 1984; 307:650–652.
55. Talle MA, Rao PE, Westberg E, Allegar N, Makowski M, Mittler RS, Goldstein G. Patterns of antigenic expression on human monocytes as defined by monoclonal antibodies. Cell Immunol 1983; 78:83–99.
56. Chakravorty SJ, Craig A. The role of ICAM-1 in *Plasmodium falciparum* cytoadherence. Eur J Cell Biol 2005; 84:15–27.
57. Wassmer SC, Lepolard C, Traore B, Pouvelle B, Gysin J, Grau GE. Platelets reorient *Plasmodium falciparum*-infected erythrocyte cytoadhesion to activated endothelial cells. J Infect Dis 2004; 189:180–189.
58. Zupancic ML, Frieman M, Smith D, Alvarez RA, Cummings RD, Cormack BP. Glycan microarray analysis of *Candida glabrata* adhesin ligand specificity. Mol Microbiol 2008; 68:547–559.
59. Prakobphol A, Genbacev O, Gormley M, Kapidzic M, Fisher SJ. A role for the L-selectin adhesion system in mediating cytotrophoblast emigration from the placenta. Dev Biol 2006; 298:107–117.
60. Cooke BM, Rogerson SJ, Brown GV, Coppel RL. Adhesion of malaria-infected red blood cells to chondroitin sulfate A under flow conditions. Blood 1996; 88:4040–4044.
61. Mitoma J, Miyazaki T, Sutton-Smith M, Suzuki M, Saito H, Yeh JC, Kawano T, Hindsgaul O, Seeberger PH, Panico M, Haslam SM, Morris HR, et al. The N-glycolyl form of mouse sialyl Lewis X is recognized by selectins but not by HECA-452 and FH6 antibodies that were raised against human cells. Glycoconj J 2009; 26:511–523.
62. Prakobphol A, Leffler H, Fisher SJ. The high-molecular-weight human mucin is the primary salivary carrier of ABH, Le(a), and Le(b) blood group antigens. Crit Rev Oral Biol Med 1993; 4:325–333.
63. Mayhew TM, Brotherton L, Holliday E, Orme G, Bush PG. Fibrin-type fibrinoid in placentae from pregnancies associated with maternal smoking: association with villous trophoblast and impact on intervillous porosity. Placenta 2003; 24:501–509.
64. Garcia-Lloret MI, Winkler-Lowen B, Guilbert LJ. Monocytes adhering by LFA-1 to placental syncytiotrophoblasts induce local apoptosis via release of TNF-alpha. A model for hematogenous initiation of placental inflammations. J Leukoc Biol 2000; 68:903–908.
65. Fried M, Muga RO, Misore AO, Duffy PE. Malaria elicits type 1 cytokines in the human placenta: IFN-gamma and TNF-alpha associated with pregnancy outcomes. J Immunol 1998; 160:2523–2530.
66. Chaudhuri S, Lowen B, Chan G, Davey A, Riddell M, Guilbert LJ. Human cytomegalovirus interacts with toll-like receptor 2 and CD14 on syncytiotrophoblasts to stimulate expression of TNFalpha mRNA and apoptosis. Placenta 2009; 30:994–1001.
67. Chan G, Guilbert LJ. Ultraviolet-inactivated human cytomegalovirus induces placental syncytiotrophoblast apoptosis in a Toll-like receptor-2 and tumour necrosis factor-alpha dependent manner. J Pathol 2006; 210: 111–120.
68. Muthusamy A, Achur R, Valiyaveettil M, Botti J, Taylor D, Leke R, Gowda D. Chondroitin sulfate proteoglycan but not hyaluronic acid is the receptor for the adherence of *Plasmodium falciparum*-infected erythrocytes in human placenta and infected red blood cell adherence up-regulates the receptor expression. Am J Pathol 2007; 170:1989–2000.
69. Muthusamy A, Achur RN, Bhavanandan VP, Fouda GG, Taylor DW, Gowda DC. *Plasmodium falciparum*-infected erythrocytes adhere both in the intervillous space and on the villous surface of human placenta by binding to the low-sulfated chondroitin sulfate proteoglycan receptor. Am J Pathol 2004; 164:2013–2025.
70. Achur RN, Valiyaveettil M, Alkhalil A, Ockenhouse CF, Gowda DC. Characterization of proteoglycans of human placenta and identification of unique chondroitin sulfate proteoglycans of the intervillous spaces that mediate the adherence of *Plasmodium falciparum*-infected erythrocytes to the placenta. J Biol Chem 2000; 275:40344–40356.
71. Maubert B, Fievet N, Tami G, Boudin C, Deloron P. Cytoadherence of *Plasmodium falciparum*-infected erythrocytes in the human placenta. Parasite Immunol 2000; 22:191–199.
72. Kristoffersen EK. Placental Fc receptors and the transfer of maternal IgG. Transfus Med Rev 2000; 14:234–243.
73. Simister NE, Story CM. Human placental Fc receptors and the transmission of antibodies from mother to fetus. J Reprod Immunol 1997; 37:1–23.
74. Pouvelle B, Matarazzo V, Jurzynski C, Nemeth J, Ramharter M, Rougon G, Gysin J. Neural cell adhesion molecule, a new cytoadhesion receptor

for *Plasmodium falciparum*-infected erythrocytes capable of aggregation. Infect Immun 2007; 75:3516–3522.
75. Craig A, Scherf A. Molecules on the surface of the *Plasmodium falciparum* infected erythrocyte and their role in malaria pathogenesis and immune evasion. Mol Biochem Parasitol 2001; 115:129–143.
76. Zhou Y, Fisher SJ, Janatpour M, Genbacev O, Dejana E, Wheelock M, Damsky CH. Human cytotrophoblasts adopt a vascular phenotype as they differentiate. A strategy for successful endovascular invasion? J Clin Invest 1997; 99:2139–2151.
77. King A, Loke YW. Differential expression of blood-group-related carbohydrate antigens by trophoblast subpopulations. Placenta 1988; 9: 513–521.
78. Jones CJ, Owens S, Senga E, van Rheenen P, Faragher B, Denton J, Brabin BJ. Placental expression of alpha2,6-linked sialic acid is upregulated in malaria. Placenta 2008; 29:300–304.
79. Winn VD, Haimov-Kochman R, Paquet AC, Yang YJ, Madhusudhan MS, Gormley M, Feng KT, Bernlohr DA, McDonagh S, Pereira L, Sali A, Fisher SJ. Gene expression profiling of the human maternal-fetal interface reveals dramatic changes between midgestation and term. Endocrinology 2007; 148:1059–1079.